Appl. Phys. B 72, 377–380 (2001) / Digital Object Identifier (DOI) 10.1007/s003400000527

Applied Physics B
Lasers
and Optics

Rapid communication

Spatial solitons in a semiconductor microresonator

V.B. Taranenko[1], **I. Ganne**[2], **R. Kuszelewicz**[2], **C.O. Weiss**[1,*]

[1] Physikalisch-Technische Bundesanstalt, 38116 Braunschweig, Germany
[2] Centre National d'Etudes de Telecommunication, BP107, 92225 Bagneux, France

Received: 17 November 2000/Published online: 13 December 2000 –

Abstract. We show experimentally the existence of bright and dark spatial solitons in a passive quantum-well-semiconductor resonator of large Fresnel number with mixed absorptive defocusing nonlinearity. Several of the solitons can exist simultaneously as required for applications.

PACS: 42.65.Sf; 42.65.Pc; 47.54.+r

We have recently shown the existence of spatial solitons in a variety of active nonlinear optical resonators [1–3], along with the control of the soliton motion by optical gradient forces [4]. The possibility of the existence of such spatial solitons in semiconductor resonators has recently been investigated in some detail theoretically [5, 6], motivated by, among other things, the possible use of these structures as fast mobile information carriers in new types of information processing [7]. Bright and dark solitons were predicted. In a recent paper [8] we have reported on pattern formation in such semiconductor microresonators which included the first evidence of structure localisation in a regime of reactive defocusing nonlinearity. In this letter we show that bright and dark solitons exist in semiconductor microresonators with absorptive/defocusing nonlinearity [9].

The semiconductor resonator used for the measurements consists of flat Bragg mirrors of about 99.7% reflectivity with 18 $GaAs/Ga_{0.5}Al_{0.5}As$ quantum wells between them. Such resonators show optical bistability when driven by a coherent field [10] so that they could support spatial solitons. The optical resonator length is approximately 3 μm, the area about 2 cm^2. Across this area the resonator wavelength varies, so that one can work from the dispersive range (wavelengths longer than the gap wavelength) to well within the absorption band. The resonator was optimized for dispersive optical bistability, for which reason the absorption of the semiconductor material is too high for pure absorptive bistability at the bandgap wavelength, where the most stable solitons are predicted.

Our previous experiments in the reactive bistability range had shown local switching in clusters of bright spots. Such bright spot clusters appear already through linear filtering of light scattered in the material by the high finesse resonator [11]. The resulting structured field prohibits the formation of unperturbed, independent spatial solitons. We worked, therefore, closer to the band gap wavelength where absorption is larger and resonator finesse, consequently, smaller, in order to avoid structuring of the field ($\lambda = 860$ nm, ≈ 10 nm in wavelength above the bandgap and 5 nm above the exciton line).

The experimental set up (Fig. 1) is conceptually simple. Light from a $Ti{:}Al_2O_3$ laser irradiates the resonator sample in an area of 40 μm diameter and with an intensity up to the kW/cm^2 range as required for saturating the semiconductor material. As the substrate of the sample is opaque in the spectral range of interest, the light reflected from the sample is observed. In order to limit thermal effects in the sample, the

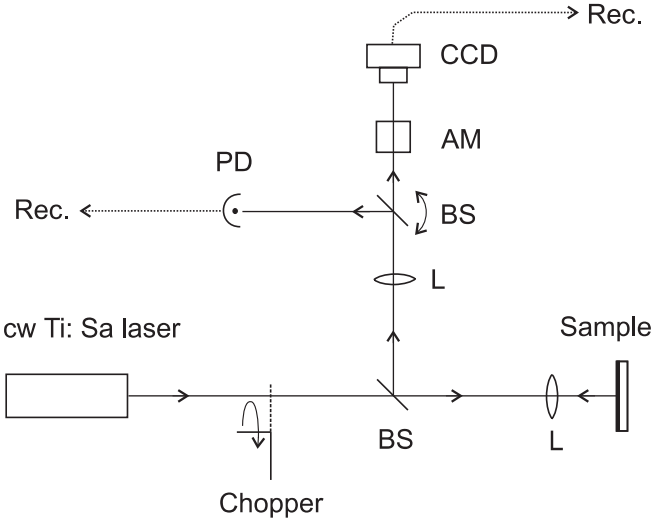

Fig. 1. Optical arrangement (BS, beamsplitter; L, lens; AM, electro-optic nanosecond shutter; PD, photodiode; CCD, camera). Change of orientation of BS allows us to image different locations on the sample onto the PD

*Corresponding author.

measurements are done during a time of a few microseconds. The laser light is admitted to the sample for about 5 μs, repeated every 1 ms, through a mechanical light chopper. The light reflected from the sample is imaged onto a CCD camera for recording 2-dimensional images. A fast amplitude modulator in front of the camera ('shutter') allows us to take snapshots with exposure times down to 10 ns. The shutter is triggered after a variable delay with respect to the beginning of the sample illumination. Thus, the evolution in time of the 2D intensity distribution of the reflected light can be followed by varying the delay.

Part of the reflected light is directed, using a beamsplitter (BS), to a fast photodiode which records the intensity at a particular point of the illuminated sample area. Recording successively the intensity as a function of time on points on a diameter of the illuminated area allows us to construct 'streak' (x, t) images representing the dynamics in the case of circularly symmetric dynamics.

Optical 'objects' (e.g. spatial intensity variations) in the light field move according to the field gradients in phase and intensity [4]. Thus, as long as there are well-defined gradients in the field, the time evolution of the 2D field is reproducible in each successive illumination. Consequently, averaging over several illuminations is possible to increase the signal/noise ratio. The CCD camera in the usual TV format reads out one frame every 40 ms, i.e. it averages 40 illuminations. For the finite extinction ratio of the electro-optical modulator (300) we used a shutter aperture time of 50 ns. The latter can be chosen by the length of a Blumlein line driving the electro-optical modulator.

Figure 2 shows switched structures as they form spontaneously at different detunings $\delta\lambda$ of laser wavelength from the resonator wavelength. Figure 2a is simply a domain switched to high transmission in the central part of the Gaussian illumination beam. The domain diameter is evidently given by the beam power. It is surrounded by a switching front at the contour of the Maxwellian intensity [12]. At moderate detuning (Fig. 2b) a sharp bright (in reflection) structure forms on the switched background. At larger detuning (Fig. 2c) a dark structure forms on the unswitched background. The bright and dark structures of Fig. 2b and c appear as predicted for dark and bright solitons, respectively, in [5, 6]. They keep their size and shape when the illumination is increased, up to a certain power, beyond which more than one of these structures appear (Fig. 6).

Figure 3 shows details of the formation of the bright soliton. Figure 3a gives the incident and reflected intensity at the location of the bright soliton and 3b gives the reflectivity on a diameter of the illuminated area in a grey code. At 1.3 μs (arrow) the resonator switches to high transmission (low reflection). The switched area then contracts relatively slowly to the stable structure Fig. 2c, which exists after $t \approx 3.0$ μs.

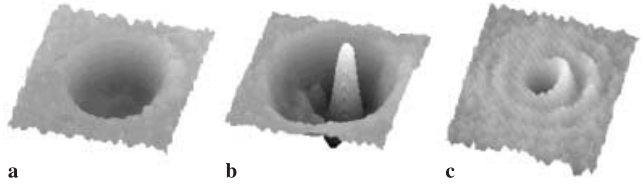

Fig. 2. Switched structures: reflectivity (reflected light/incident light) of the sample: **a** switched domain (limited by a contour of Maxwellian intensity) at $\delta\lambda = -0.45$ nm, power 75 mW; **b** dark soliton in the switched domain (bright spot in reflection) at $\delta\lambda = -0.60$ nm, power 360 mW;**c** bright soliton on the unswitched background (dark spot in reflection) at $\delta\lambda = -0.75$ nm, power 160 mW. Parameters: $\lambda = 860$ nm; diameter of illuminated area, 40 μm

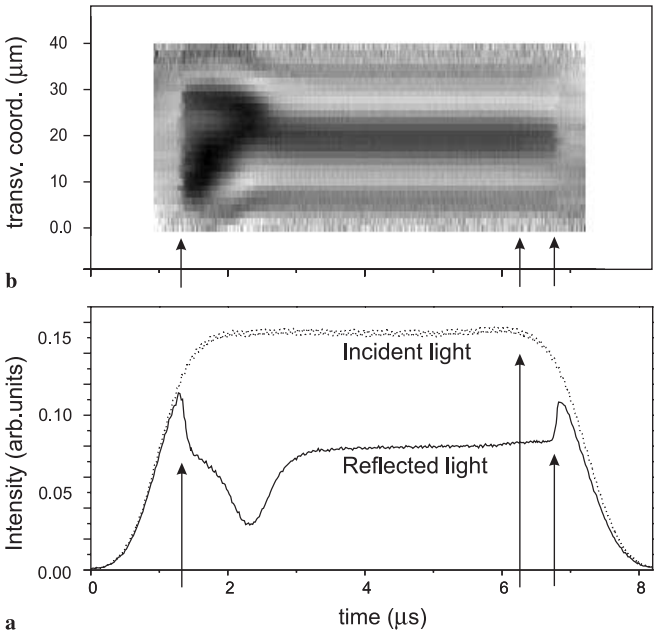

Fig. 3. Formation of bright soliton corresponding to Fig. 2c: **a** incident (*dotted*) and reflected (*solid*) light intensity at the center of the Gaussian illuminating beam; **b** reflectivity vs. time on a cross-section of illuminated area in a grey code. The switched area contracts to form a stable soliton whose diameter is constant in time and independent of illuminating intensity. Intensity unit as in Figs. 4 and 5

We interpret this particular formation of a soliton by temperature effects in the sample. After the resonator switches to low reflection its internal field, and with it the dissipation, is high. A rising temperature decreases the band gap energy [13] and therefore shifts the bistable resonator characteristic towards higher intensity. Thus, the basin of attraction for solitons which is located near the switch-off intensity [5] is shifted to the incident intensity, whereupon a soliton can form. Evidently, for different parameters the shift can be substantially larger or smaller than the width of the bistability loop, in which case no stable soliton can appear. We note that in the absence of thermal effects (good heatsinking of the sample) solitons would not appear spontaneously but would have to be switched on by local pulsed light injection.

The stable structure, Figs. 2c and 3b after $t \approx 3.0$ μs, shows the characteristic features of a spatial soliton:

(i) Stable diameter in time.
(ii) Size of 10 μm as expected from model calculations [5, 6].
(iii) Surrounded by characteristic rings due to the 'oscillating tails' of the switching front [14].
(iv) Robustness: From $t \approx 6.3$ μs in Fig. 3 (arrow) the incident light intensity drops. In spite of this change of illumination, the brightness of the structure as well as its size remain constant until the time it switches off abruptly ($t \approx 6.8$ μs (arrow)). Such immunity against ex-

ternal parameter variation would seem characteristic for a nonlinearly stabilized structure.

(v) We note the fast switch-off of the structure at $t \approx 6.8\,\mu s$. The structure disappears abruptly at a certain intensity, in a manner suggesting a subcritical process. This allows us to conclude that the nonlinearity is 'fast' (electronic). A slow (e.g. thermal) nonlinearity would not allow such abrupt disappearance of the structure.

(vi) Bistability, a fundamental property of such solitons, was also experimentally confirmed [15].

Due to properties (i)–(vi) we can indeed identify the structure with a bright soliton based on a fast nonlinearity.

The formation of the dark soliton Fig. 2b is illustrated in Fig. 4. When the illumination intensity is increased, the resonator switches (arrow, at $t \approx 0.7\,\mu s$). After this the intensity is further increased substantially over that in Figs. 2c and 3 so that the intensity is above the attraction basin of bright solitons. At a high enough intensity, again after a longer transient, the dark soliton (bright in reflection) forms, somewhat off the beam center (Fig. 2b). The dark structures marked by arrows correspond to some structure, non-symmetric with respect to the illuminating beam center, such as is visible in Fig. 2b. Figure 4b shows that the soliton moves in the observation plane and is perpendicular to it, as recognizable from the 2D snapshots on top. The reduction of the brightness of the soliton with time in Fig. 4b is due partly to the motion of the soliton perpendicularly to the plane of Fig. 4b. Partly it appears that the shift of the bistable resonator characteristic, due to dissipation, toward higher intensity, reduces the soliton brightness in time. This means that the dark soliton must not always be stable (it can actually be pulsing, due to the combined action of electronic nonlinearity and thermal shift of the characteristic; see Fig. 5b) and would only be stable for good heatsinking.

It is noteworthy that the peak intensity of the soliton (Fig. 4a) is higher than the incident intensity. This means that the soliton collects and concentrates light from its surrounding.

Figure 5 gives an overview of the intensity ranges for existence of bright and dark solitons. Intensities are measured at the location of the solitons. Figure 5a corresponds to the bright soliton Fig. 2c, Fig. 5b corresponds to a pulsing soliton, and Fig. 5c to a stable dark soliton (living longer than the illumination duration).

Figure 6 finally shows that (in spite of the small illumination area which is limited by gradients of the sample) two bright solitons (Fig. 6a) and two and three dark solitons (Fig. 6b and c) can exist simultaneously. Up to five coexisting dark solitons were observable.

Concluding, we find for light wavelength corresponding to absorptive defocusing nonlinearity and for large (blue) detuning of light from resonance, the existence of bright and dark spatial resonator solitons compatible with recent theoretical predictions.

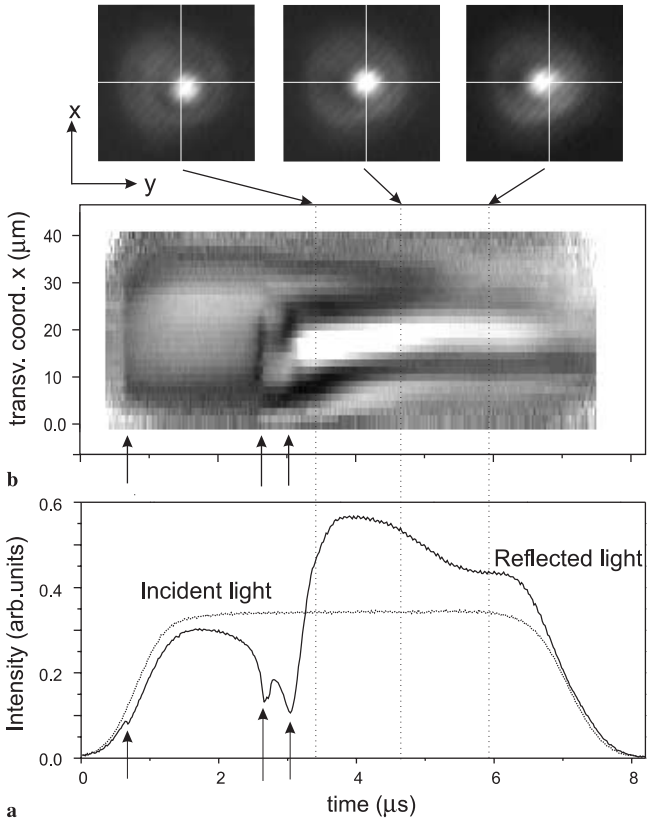

Fig. 4. Formation of a dark soliton corresponding to Fig. 2b. **a** incident (*dotted*) and reflected (*solid*) intensity at the center of the illuminating beam; **b** reflectivity versus time on a cross-section of the illuminated area in a grey code. After some structure formation (*arrows*) a dark soliton develops. Motion of the soliton is illustrated by snapshots on top. Intensity unit as in Figs. 3 and 5

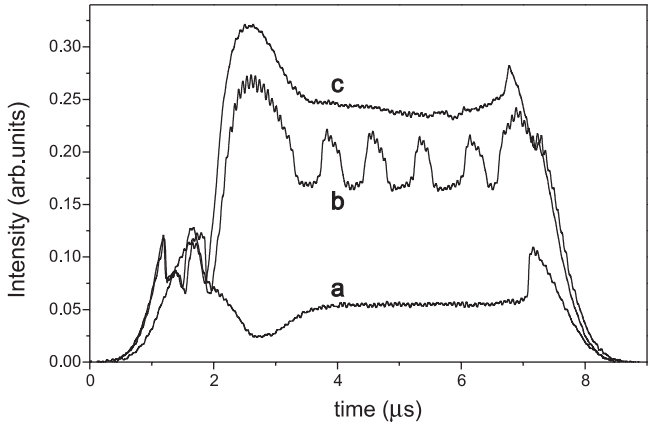

Fig. 5. Reflected light intensity measured at the center of the Gaussian illumination beam. Parameters: $\delta\lambda = -0.8$ nm; power, 130 mW (a), 245 mW (b), 270 mW (c); (b) shows the regenerative pulsing resulting from the combined effects of thermal shift of the resonator characteristic (due to thermal shift of bandgap) and electronic nonlinearity. Intensity unit as in Figs. 3 and 4

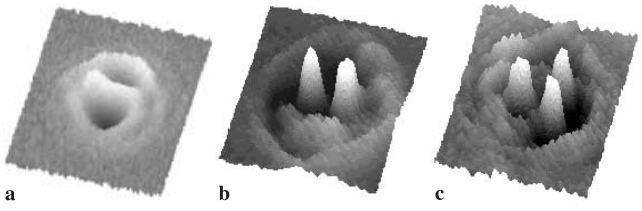

Fig. 6. Simultaneous existence of several solitons: **a** two bright solitons; **b** two dark solitons; **c** three dark solitons. Representation and coding as in Fig. 2

Acknowledgements. This work was supported by the ESPRIT LTR project PIANOS.

References

1. K. Staliunas, V.B. Taranenko, G. Slekys, R. Viselga, C.O. Weiss: Phys. Rev. A **57**, 599 (1998)
2. G. Slekys, K. Staliunas, C.O. Weiss: Opt. Commun. **149**, 113 (1998)
3. V.B. Taranenko, K. Staliunas, C.O. Weiss: Phys. Rev. Lett. **81**, 2226 (1998)
4. K. Staliunas: Phys. Rev. A **48**, 1573 (1993)
5. M. Brambilla, L.A. Lugiato, F. Prati, L. Spinelli, W.J. Firth: Phys. Rev. Lett. **79**, 2042 (1997); L. Spinelli, G. Tissoni, M. Brambilla, F. Prati, L.A. Lugiato: Phys. Rev. A **58**, 2542 (1998); G. Tissoni, L. Spinelli, M. Brambilla, T. Maggipinto, I.M. Perrini, L.A. Lugiato: J. Opt. Soc. Am. B **16**, 2083 (1999)
6. D. Michaelis, U. Peschel, F. Lederer: Phys. Rev. A **56**, R3366 (1997)
7. W.J. Firth, G.K. Harkness: Asian J. Phys. **7**, 665 (1998)
8. V.B. Taranenko, I. Ganne, R. Kuszelewicz, C.O. Weiss: Phys. Rev. A **61**, 63 818 (2000)
9. V.B. Taranenko, I. Ganne, R. Kuszelewicz, C.O. Weiss: Los Alamos Preprint Server nlin. PS/0001056 V.B. Taranenko, C.O. Weiss: post-deadline paper CLEO/IQEC, San Francisco, 11 May 2000
10. B.G. Sfez, J.L. Oudar, J.C. Michel, R. Kuszelewicz, R. Azoulay: Appl. Phys. Lett. **57**, 1849 (1990); I. Abram, S. Iung, R. Kuszelewicz, G. LeRoux, C. Licoppe, J.L. Oudar: Appl. Phys. Lett. **65**, 2516 (1994)
11. A. Berzanskis, K. Staliunas, private communication
12. N.N. Rosanov: Prog. Opt. **35**, 1 (1996); N.N. Rosanov, G.V. Khodova: J. Opt. Soc. Am. B **7**, 1057 (1990)
13. T. Rossler, R.A. Indik, G.K. Harkness, J.V. Moloney, C.Z. Ning: Phys. Rev. A **58**, 3279 (1998)
14. W.J. Firth, A.J. Scroggie: Phys. Rev. Lett. **76**, 1623 (1996)
15. V.B. Taranenko, C.O. Weiss: Los Alamos Preprint Server nlin. PS/0003004